1 μs tunable delay using parametric mixing and optical phase conjugation in Si waveguides

Yitang Dai,[1] Xianpei Chen,[1] Yoshitomo Okawachi,[1] Amy C. Turner-Foster,[2] Mark. A. Foster,[1] Michal Lipson, [2] Alexander L. Gaeta,[1] and Chris Xu[1]

[1]*School of Applied and Engineering Physics, Cornell University, Ithaca, NY 14853*
[2]*School of Electrical and Computer Engineering, Cornell University, Ithaca, NY 14853*
yd82@cornell.edu

Abstract: We demonstrate continuously tunable optical delays as large as 1.1 μs range for 10 Gb/s NRZ optical signals based on four-wave mixing (FWM) process in silicon waveguide. The large delay range is made possible by a novel wavelength-optimized optical phase conjugation scheme, which allows for tunable dispersion compensation to minimize the residual group-velocity dispersion (GVD) for the entire tuning range.

OCIS codes: (190.4380) Nonlinear optics, four-wave mixing; (190.4390) Nonlinear optics, integrated optics

References and links

1. M. K. Dhodhi, S. Tariq, and K. A. Saleh, "Bottlenecks in next generation DWDM-based optical networks," Comput. Commun. **24**, 1726–1733 (2001).
2. S. J. B. Yoo, "Optical packet and burst switching technologies for the future photonic internet," J. Lightwave Technol. **24**, 4468–4492 (2006).
3. E. Choi, J. H. Na, Y. Ryu, G. Mudhana, and B. H. Lee, "All-fiber variable optical delay line for applications in optical coherence tomography: feasibility study for a novel delay line," Opt. Express **13**, 1334–1345 (2005).
4. J. L. Corral, J. Marti, J. M. Fuster, and R. I. Laming, "True time-delay scheme for feeding optically controlled phased-array antennas using chirped-fiber gratings," Photon. Technol. Lett. **9**, 1529–1531 (1997).
5. G. N. Pearson, K. D. Ridley, and D. V. Willetts, "Chirp-pulse-compression three dimensional lidar imager with fiber optics," Appl. Opt. **44**, 257–265 (2005).
6. Y. Han and B. Jalali, "Photonic time-stretched analog-to-digital converter: Fundamental concepts and practical considerations," J. Lightwave Technol. **21**, 3085–3103 (2003).
7. R. Ramaswami and K. N. Sivarajan, Optical Networks: A Practical Perspective (Morgan Kaufmann, 2002).
8. R. W. Boyd and D. J. Gauthier, "'Slow' and 'fast' light," Progress in Optics 43, edited by E. Wolf (Elsevier, Amsterdam, 2002), Chap. 6, p. 497–530.
9. R. W. Boyd, D. J. Gauthier, and A. L. Gaeta, "Applications of slow light in telecommunications," Opt. Photon. News **17**, 18–22 (2006).
10. M. Burzio, P. Cinato, R. Finotti, P. Gambini, M. Puleo, E. Vezzoni, and L. Zucchelli, "Optical cell synchronization in an ATM optical switch," in Proc. ECOC '94, Florence, Italy, 2, 581–584 (1994).
11. L. Zucchelli, M. Burzio, and P. Gambini, "New solutions for optical packet delineation and synchronization in optical packet switched networks," in Proc. ECOC '96, Oslo, Norway, 3, 301–304 (1996).
12. K. Shimizu, G. Kalogerakis, K.Wong, M. Marhic, and L. Kazovsky, "Timing jitter and amplitude noise reduction by a chirped pulsed-pump fiber OPA," in Proc. OFC '03, Anaheim, USA, 1, 197–198 (2003).
13. J. van Howe and C. Xu, "Ultrafast optical delay line using soliton propagation between a time-prism pair," Opt. Express **13**, 1138–1143 (2005).
14. Y. Wang, C. Yu, L. Yan, A. E. Willner, R. Roussev, C. Langrock, M. M. Fejer, J. E. Sharping, and A. E. Gaeta, "44-ns continuously tunable dispersionless optical delay element using a PPLN waveguide with two-pump configuration, DCF, and a dispersion compensator," Photon. Technol. Lett. **19**, 861–863 (2007).
15. L. C. Christen, O. F. Yilmaz, S. R. Nuccio, X. Wu, I. Fazal, A. E. Willner, C. Langrock, and M. M. Fejer, "Tunable 105 ns optical delay for 80 Gb/s RZ-DQPSK, 40 Gb/s RZ-DPSK, and 40 Gb/s RZ-OOK signals using wavelength conversion and chromatic dispersion," Opt. Lett. **34**, 542-544 (2009).
16. J. E. Sharping, Y. Okawachi, J. van Howe, C. Xu, Y. Wang, A. E. Willner, and A. L. Gaeta, "All-optical, wavelength and bandwidth preserving, pulse delay based on parametric wavelength conversion and dispersion," Opt. Express **13**, 7872–7877 (2005).

#106927 - $15.00 USD Received 29 Jan 2009; revised 1 Apr 2009; accepted 8 Apr 2009; published 13 Apr 2009

17. Y. Okawachi, M. A. Foster, X. Chen, A. C. Turner-Foster, R. Salem, M. Lipson, C. Xu, and A. L. Gaeta, "Large tunable delays using parametric mixing and phase conjugation in Si nanowaveguides," Opt. Express **16**, 10349-10357 (2008).
18. E. Myslivets, N. Alic, J. R. Windmiller, R. M. Jopson, and S. Radic, "400 ns continuously tunable delay of 10 Gbps intensity modulated optical signal," Photon. Technol. Lett., **21**, 4, 251-253 (2009).
19. M. A. Foster, A. C. Turner, R. Salem, M. Lipson, and A. L. Gaeta, "Broad-band continuous-wave parametric wavelength conversion in silicon nanowaveguides," Opt. Express **15**, 12,949–12,958 (2007).
20. S. Namiki, "Wide-band and –range tunable dispersion compensation through parametric wavelength conversion and dispersion optical fibers," J. Lightwave Technol. **26**, 28-35 (2008).
21. A. Yariv, D. Fekete, and D. M. Pepper, "Compensation for channel dispersion by nonlinear optical phase conjugation," Opt. Lett. **4**, 52–54 (1979).
22. S. Ayotte, S. Xu, H. Rong, O. Cohen, and M. J. Paniccia, "Dispersion compensation by optical phase conjugation in silicon waveguide," Electron. Lett. **43**, 1037–1039 (2007).
23. G. P. Agrawal, Nonlinear Fiber Optics (Academic Press, Boston, 1989).
24. B. G. Lee, A. Biberman, M. A. Foster, A. C. Turner, M. Lipson, A. L. Gaeta, and K. Bergman, "Bit-error-rate characterization of Silicon four-wave-mixing wavelength converters at 10 and 40 Gb/s," CLEO 2008, paper CPDB4.

1. Introduction

The capability of buffering or delaying information is highly desired in communication networks. Specific applications include network buffering, data synchronization, and time-division multiplexing. While information is transmitted using optical fibers in current communication networks, components for data processing requires optical/electronic conversion of information, creating a bottleneck for further increasing the data transmission rate [1]. The ability to create precise all-optical delays, i.e., being able to control the arrival times of data streams on the physical level, is then a critical requirement. Rather than discrete optical delays that can be generated by combining a series of fixed delay lines with different amounts of delay in parallel [2], fine and continuous tuning of the delay is required as the data rate increases. The development of tunable optical delay lines is also important for other applications such as optical coherence tomography [3], optical control of phased array antennas for radio frequency communication [4], light detection and sensing (LIDAR) [5], optical sampling [6], and pattern correlation [7].

Recent research efforts include the ability to reduce the speed of an optical signal by several orders of magnitude, which takes advantage of the rapidly-varying refractive index that accompanies an optical resonance [8]. However, the maximum delay that can be generated in practical slow-light delay lines has been limited to a few pulse widths [9]. An alternative technique for generating tunable delays utilizes wavelength conversion and dispersion [10-16]. This scheme takes advantage of the group-velocity dispersion (GVD) in an optical fiber for generating a wavelength-dependent optical delay. The wavelength of the input signal is shifted and injected into a medium with a large GVD, which generates a delay with respect to the initial unshifted pulse. The total delay is approximately a product of the GVD parameter D, the length of the dispersive fiber L_d, and the wavelength shift $\Delta\lambda$. To achieve large delays, however, the necessarily large GVD inevitably results in severe distortions to the delayed signal. The use of the inherent temporal phase conjugation associated with four-wave mixing (FWM) can overcome the GVD-induced pulse broadening and allows us to further extend the maximum achievable delay [17]. Such scheme consists of three stages: a dispersive fiber, a FWM wavelength conversion, and a second dispersive fiber which is typically the same fiber as the first stage. 243-ns delay for a 10-Gb/s NRZ signal has been demonstrated based on this design. However, since dispersive fibers also possess non-vanishing higher order dispersion, the large residual dispersion between the original and the converted wave limits the maximum delay range. A new scheme including a partial dispersion slope cancellation is proposed, and the maximum tunable delay range has been extended to 400 ns at 10 Gb/s [18]. Unfortunately, residual dispersion at the output signal of more than 200 ps/nm still exists. Such a scheme has limited potential for further improvement in delay range and data rate.

#106927 - $15.00 USD Received 29 Jan 2009; revised 1 Apr 2009; accepted 8 Apr 2009; published 13 Apr 2009

In this paper we propose a novel tunable parametric optical delay system based on wavelength-optimized optical phase conjugation, which allows one half of the delay system to serve simultaneously as a tunable dispersion compensator with only fixed dispersion elements. Zero residual GVD at the output signal can be obtained throughout the delay range. Optical phase conjugation is realized in silicon waveguides. For fiber-based optical parametric schemes, pump modulation is necessary in order to suppress stimulated Brillouin scattering (SBS), which distorts the output if a single pump is used. Since the silicon waveguides do not exhibit SBS, a single CW pump can be used without any phase modulation [19]. This paper reports, for the first time to the best of our knowledge, continuously tunable optical delays at 10 Gb/s with greater than a 1-μs delay range.

2. Theory

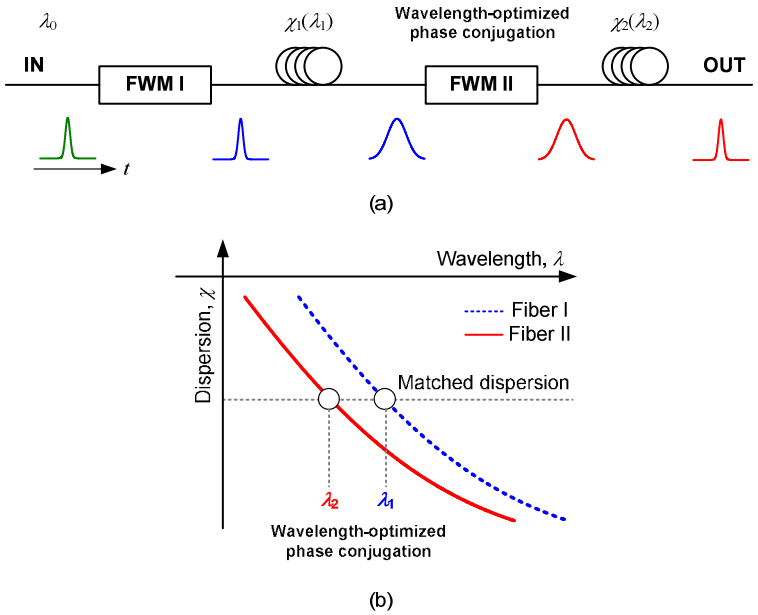

Fig. 1. (a) Delay generator using two wavelength conversions via FWM and two dispersion links. (b) The principle of zero residual dispersion based on the wavelength-optimized optical phase conjugation.

The concept of the proposed system is illustrated in Fig. 1. The input signal is first wavelength-converted from λ_0 to λ_1 (can be with or without phase conjugation) and then transmitted along fiber I with a dispersion function $\chi_1(\lambda)$. After the second wavelength conversion to λ_2 (with phase conjugation), the signal is transmitted along the second dispersive link, fiber II with dispersion function $\chi_2(\lambda)$. The principle of zero residual dispersion at the output signal is shown in Fig. 1(b). As a result of the phase conjugation process in FWM II, the signal broadening effect induced by fiber I can be compensated by the dispersion in fiber II. In order to realize zero residual dispersion, the total dispersion that the signal experiences in the two fibers are required to be the same, that is,

$$\chi_1(\lambda_1) = \chi_2(\lambda_2). \tag{1}$$

In order to achieve continuously tunable delays, λ_1 must be tuned within the achievable wavelength conversion range. The proposed design requires the signal wavelength within fiber II to be determined by Eq. (1). In fact, in addition to providing dispersive delay, the second dispersive link also serves as a tunable dispersion compensator. λ_2 is the matched wavelength point. Although such a dispersion compensation scheme is similar to that reported in Ref. [20], the combination of delay generation and dispersion compensation in the same

#106927 - $15.00 USD Received 29 Jan 2009; revised 1 Apr 2009; accepted 8 Apr 2009; published 13 Apr 2009

setup is advantageous for tunable optical delays. The tunable delay in the proposed system can be expressed as

$$\tau(\lambda_1)=\int_{\lambda_{10}}^{\lambda_1}\chi_1(\lambda)d\lambda+\int_{\lambda_{20}}^{\lambda_2}\chi_2(\lambda)d\lambda\,, \tag{2}$$

where λ_{10} is the reference point, and λ_{20} and λ_2 are determined by λ_{10} and $\lambda_{1,}$ respectively, as shown in Eq. (1).

We present here a brief theoretical analysis of the phase distortion that the signal suffers in propagating through the entire delay system. Generally the dispersion function of the fiber can be expanded at a particular wavelength and described by its second order (i.e. the GVD) and higher order dispersion, i.e., β_2, β_3, β_4… Due to temporal phase conjugation after the first dispersive link and FWM II, the dispersion that the signal experiences is then effectively -$\beta_{2,1}$, $\beta_{3,1}$, -$\beta_{4,1}$…, i.e., the signs of all the even terms are changed while the odd terms are kept unchanged [21-23]. As a result, at the output of the system the phase distortion of the signal (in the frequency domain) is

$$\begin{aligned}\varphi(\Delta\omega)=&\frac{\Delta\omega^2}{2}\left[\beta_{2,2}(\omega_2)L_2-\beta_{2,1}(\omega_1)L_1\right]+\frac{\Delta\omega^3}{6}\left[\beta_{3,2}(\omega_2)L_2+\beta_{3,1}(\omega_1)L_1\right]\\&+\frac{\Delta\omega^4}{24}\left[\beta_{4,2}(\omega_2)L_2-\beta_{4,1}(\omega_1)L_1\right]+\cdots\end{aligned}, \tag{3}$$

where L_1 and L_2 are the fiber lengths, and ω_1 and ω_2 are the optical frequencies of the signal in the two fibers.

In previous work [17,18], where FWM I is not used, ω_1 is fixed at the input signal frequency and ω_2 is determined by the required delay value. Due to the non-zero higher order dispersion in the fiber, the first term in Eq. (3) is generally non-zero and dominates the phase distortion of the output signal. In order to minimize such residual GVD, a pre- or post-compensation can be used to optimize the system performance. The best value of such a pre- or post-compensation is the mean residual GVD when ω_2 is tuned through the wavelength conversion range ($\Delta\omega_C$) in order to produce the delay. When fiber I and fiber II are the same or have nearly identical dispersion properties [17, 18], for example, the maximum residual phase distortion can be estimated as

$$\varphi_{\max}(\Delta\omega)=\left|\frac{\Delta\omega^2}{4}\overline{\beta_3 L}\Delta\omega_C\right|, \tag{4}$$

where $\overline{\beta_3 L}$ is the mean third order dispersion (TOD) of the two fibers, which can be large when the fiber length is long. As a result, the large GVD variation in the wavelength conversion range [$\overline{\beta_3 L}\Delta\omega_C$ in Eq. (4)] ultimately limits the achievable maximum delay range and the highest data rate the system can support.

In our proposed system, however, the first term in the phase distortion is zero throughout the wavelength conversion range when Eq. (1) is satisfied, and the dominant phase distortion is now the second term. Similarly, a pre- or post-compensation with the optimized value of the mean residual TOD can be used to minimize the phase distortion, and then the maximum residual phase distortion is

$$\varphi'_{\max}(\Delta\omega)=\left|\frac{\Delta\omega^3}{6}\overline{\beta_4 L}\Delta\omega_C\right|, \tag{5}$$

where $\overline{\beta_4 L}$ is the mean fourth order dispersion of the two fibers. Equation (5) shows that the system performance is now limited by the fourth-order dispersion instead of the TOD, which significantly increases the maximum delay range and the highest data rate that parametric delay system can support.

Equation (1) shows that $\lambda_1\equiv\lambda_2$ if the two fibers are identical, indicating wavelength-shiftless phase conjugation. Since phase conjugation is usually accompanied by wavelength conversion, three FWM stages (or FWM with polarization-multiplexed dual pumps) may be

#106927 - $15.00 USD Received 29 Jan 2009; revised 1 Apr 2009; accepted 8 Apr 2009; published 13 Apr 2009

needed for such a wavelength-shiftless scheme, which greatly increases the system complexity. Note that even in such a wavelength-shiftless phase conjugation scheme, the maximum phase distortion is still governed by Eq. (5), the same as the proposed wavelength-optimized phase conjugation with only one FWM. Thus, the proposed scheme achieves nearly identical system performance, when compared to wavelength-shiftless phase conjugation, but without the added complexity. In practice, the same DCF is usually used in the first and second dispersive link in order to maximize the achievable tunable delay range with a given fiber length. In such a case, a dispersive medium with a small dispersion value can be used before or after the DCF to slightly shift the dispersion curve of one of the dispersive links (an example is shown in section 3).

3. Experiment

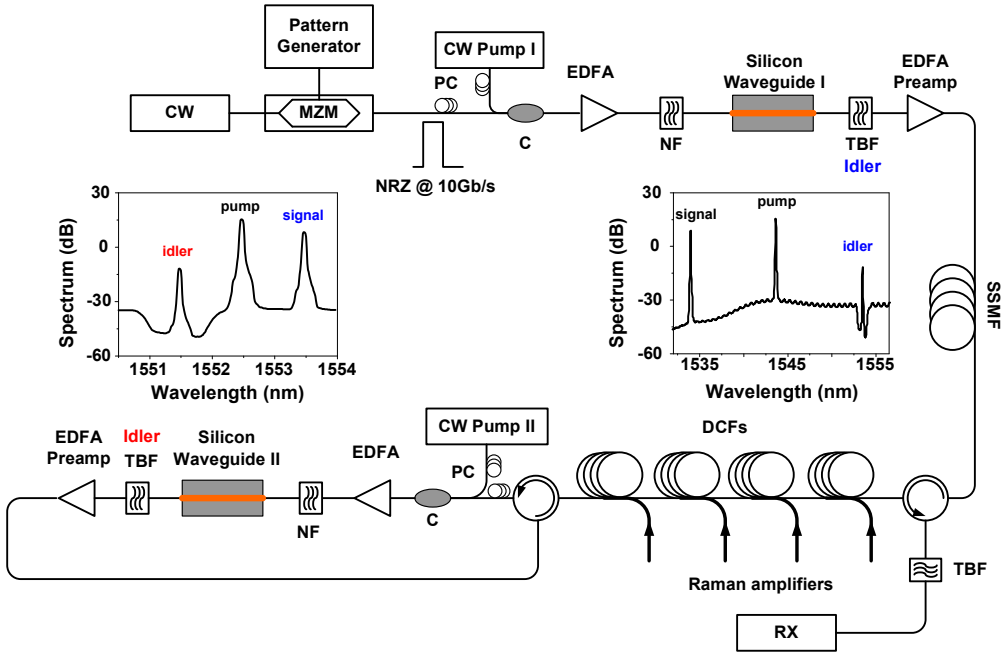

Fig. 2. Experimental setup for the delay scheme based on wavelength-optimized optical phase conjugation. C: coupler; TBF: tunable bandpass filter; SSMF: standard single mode fiber, PC: polarization controller. NF: notch filter. Each of the four Raman amplifiers consists of four semiconductor LDs. Polarization multiplexing is used to combine the pump diodes, and the pump power for each amplifier is 23 dBm. The spectrum after each waveguide is inset. The resolution in the measurement is 0.1 nm.

The experimental setup is shown in Fig. 2. A CW DFB laser centered at 1534 nm is modulated using a pattern generator and a Mach-Zehnder modulator to generate NRZ signal at 10 Gb/s. The signal is combined with CW pump I and amplified to 250 mW. The signal power is kept approximately 5 dB below the pump power for optimal wavelength conversion. The signal and pump are then coupled into a silicon (Si) waveguide for the first wavelength conversion. The Si waveguide is 1.1-cm long and has a cross section of 600 nm by 300 nm. By tuning the wavelength of pump I, the wavelength of the idler can be tuned continuously from 1535.5 nm to 1572 nm, limited entirely by the gain flattening range of the EDFA. The on-off conversion efficiency is around -20 dB and the output OSNR is around 35 dB after conversion. The OSNR performance is improved from previous experiments [17] by using a notch filter before the waveguide, which eliminates the ASE noise at the band where the idler will be generated. Custom notch filters based on fiber Bragg gratings are used in the following BER test experiment. A continuously tunable notch filter (e.g., OTF-960 from Santec) is also commercial available. A DCF (four 15 km spools of HFDK, OFS Denmark) with a total

#106927 - $15.00 USD Received 29 Jan 2009; revised 1 Apr 2009; accepted 8 Apr 2009; published 13 Apr 2009

dispersion of approximately -15 ns/nm at 1550 nm and 40 dB loss is used to achieve a large tunable delay range. Since the same DCF is used for both dispersion links, a 5-km SSMF is used before the first circulator to shift the first dispersion curve by 85 ps/nm. The signal after the second circulator is wavelength shifted again by FWM II (the setup for FWM II is identical to that of FWM I). The wavelength shift in FWM II is determined by Eq. (1). After FWM II, the idler is pre-amplified, sent back into the second circulator, through the same DCF, and into the first circulator. Finally, the output is filtered and detected by a standard 10-Gb/s receiver. Four broadband Raman amplifiers are used within the DCF to achieve lossless transmission in the DCF throughout the wavelength conversion range. If it is required, a third wavelength conversion stage can be implemented at the output to convert the signal to the desired wavelength [16]. This third wavelength conversion will have no impact on the dispersion management and the delay range. It has been demonstrated previously that the additional wavelength conversion based on the Si waveguide will result in a small power penalty (~ 1 dB) to the system [24].

The signal delays at various conversion wavelengths λ_1 can be directly observed by an oscilloscope when a long, slow data pattern with 100 Mb/s is used. As shown in Fig. 3, a tunable delay range of 1088 ns is achieved when λ_1 is tuned over a range of 36.5 nm. Since the tuning of λ_2 acts as a tunable dispersion compensator to cancel the phase distortion for the output signal, we obtain a much larger tunable delay range than in previous demonstrations [17, 18]. We are currently limited by the gain flattening range of the EDFAs in our system. The maximum wavelength conversion range, and thus, the maximum delay range allowed by the Si waveguide and the dispersion management scheme is significantly beyond what we have demonstrated.

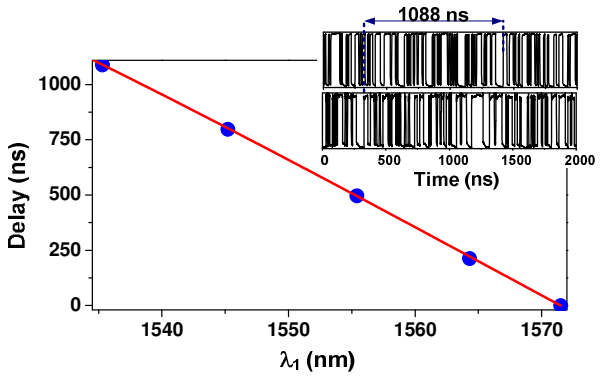

Fig. 3. Measured delay as a function of λ_1. Inset: the measured delay for λ_1 = 1535.5 nm (top) and 1572 nm (bottom).

Figure 4 shows the bit-error-rate tests and the eye diagrams measured at the two edges and center point in the delay generator. A $(2^{23}-1)$ pseudo-random bit sequence (PRBS) is used. The measured power penalty is around 3.3 to 4.5 dB for a BER of 10^{-9}. The power penalty can be attributed in part to the degradation of the optical signal-to-noise ratio (OSNR) in the wavelength conversion process. Both linear propagation loss and nonlinear loss due to two-photon absorption and free-carrier absorption reduce the efficiency of the FWM process in the silicon waveguides.

#106927 - $15.00 USD Received 29 Jan 2009; revised 1 Apr 2009; accepted 8 Apr 2009; published 13 Apr 2009

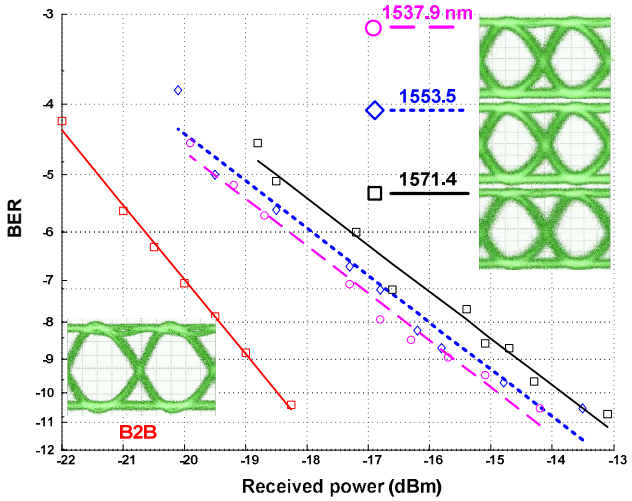

Fig. 4. Measured eye diagrams and BER curves of back-to-back (B2B) signals and delayed signals when λ_1 is at different wavelengths.

The PMD of the system is estimated to be 6 ps, which shows no impact on a 10 Gb/s signal, but it will distort the signal at much higher data rate. A possible solution for this issue is to shorten the fiber length while enlarging the wavelength tuning range to keep the same tunable delay range. Furthermore, the polarization-dependent response of the Si-waveguide can be mitigated by two orthogonal pumps. For example, by injecting a single pump into both polarization states of the waveguide, we achieved wavelength conversion efficiency with less than 0.5 dB polarization sensitivity.

4. Conclusion

We proposed a novel parametric tunable delay system with a wavelength-optimized optical phase conjugation that allows for tunable dispersion compensation. Theoretical analysis showed that zero GVD can be obtained throughout the tuning range and predicts the potential of an even larger range of delays and operation at higher data rates. More than 1 μs continuously tunable delay was experimentally demonstrated at 10 Gb/s.

Acknowledgments

The authors gratefully acknowledge support from the DARPA MTO POPS Program. We also acknowledge valuable discussions with Prof. Keren Bergman and her research group at Columbia. OFS Denmark is acknowledged for loaning parts of the HFDK.

#106927 - $15.00 USD Received 29 Jan 2009; revised 1 Apr 2009; accepted 8 Apr 2009; published 13 Apr 2009